

EFFECTS OF OXY JET IN CROSS-FLOW ON THE COMBUSTION INSTABILITY AND NO_x EMISSIONS IN LEAN PREMIXED FLAME

by

Chengfei TAO and Hao ZHOU*

State Key Laboratory of Clean Energy Utilization, Zhejiang University, Hangzhou, China

Original scientific paper

<https://doi.org/10.2298/TSCI201215178T>

Combustion instability and NO_x emission are crucial factors for modern gas turbine combustors, which seriously hampers the research and development of advanced combustors. To eliminate combustion instability and NO_x emissions simultaneously, effects of the oxy (CO₂/O₂, N₂/O₂, Ar/O₂, and He/O₂) jet in cross-flow on combustion instability and NO_x emissions are experimentally studied. In this research, the flow rate and oxygen ratio of the combustor are varied to evaluate the control effectiveness. Results denotes that all the four oxyfuel gas: CO₂/O₂, N₂/O₂, Ar/O₂, and He/O₂, could suppress combustion instability and NO_x emissions. The CO₂/O₂ dilution can achieve a better damping results than the other three cases. There are peak values or lowest points of sound pressure amplitude as the parameter of oxy jet in cross-flow changes. Mode transition appears in both acoustic signal and CH chemiluminescence of the flame. But the turning point of mode transition is different. Under the CO₂/O₂ cases, the NO_x emission decreases from 22.3 ppm to 15.2 ppm, the damping ratio of NO_x is 40.39%. The flame shape and length were changed under different jet in cross-flow dilutions. This research could promote the application of jet in cross-flow methods on combustion instability or pollutant emissions in gas turbines.*

Key words: *combustion instability, NO_x emission, oxygen ratio, premixed flame, oxyfuel, jet in cross-flow*

Introduction

Due to its excellent performance in reducing the NO_x emissions of combustion, lean premixed combustion techniques are widely used in gas turbine engines and other industrial fields. Lean premixed combustion technology is easily troubled with the combustion instability (or thermoacoustic instability) while achieving clean combustion purpose [1]. With the continuously demand for the clean, high efficient, robust, and reliable gas turbine engines from the industrial sectors, combustion instabilities has becoming the key factors that to hinder the development of advanced combustors. Combustion instability arise from the coupling of the fluctuation sound and heat release of the unsteady flame [2]. The interaction between the flame and the sound waves will form unsteady flow oscillations in the combustion chamber [3]. The intensity and amplitude of thermoacoustic instability will continue to grow, which will damage the structure of the combustion chamber or affecting the normal combustion of the burner [4]. Thermoacoustic instability will cause serious structural damages, thermal stresses damages and abnormal phenomena such as flashback and blowout [5]. Combustion instabilities always associated with acoustic oscillations, flow/mixture oscillations and heat release rate oscillations [6].

* Corresponding author, e-mail: zhouhao@zju.edu.cn

The multidisciplinary or non-linear characteristics make the suppression and analyzing of combustion instability very challenging [7-10]. In order to better eliminate the combustion instability with lean premixed combustion technology, active and passive control methods are promoted [11, 12]. Active control method use closed-loop feedback realized the online monitoring and control of combustion instability [11]. The passive control method mainly suppresses the sound waves in the combustion chamber by sound absorption devices [12]. However, in a lean premixed combustor, combustion instability and NO_x emissions are all traditionally contradictory variables that controls the operation window of lean premixed combustion [13]. How to achieve the synchronization control of combustion instability and NO_x is very important. Neither like the traditional active control systems (which is expensive and complex) nor like the passive control methods that indirectly interfere combustion chemical reaction process. Application of microjets around the flame anchoring zones have the potential of elimination sound waves and pollutants in the combustion chamber [14]. The jet in cross-flow (JICF) method is simple and easy to implement on combustor, which can simultaneously change the chemical reaction process and the flow field of the flame. The mixing and vortex shedding process of combustion reactants can be changed at the same time.

The potential for eliminating combustion instability or NO_x emissions with the passive method of JICF have been shown in the past [13-22]. Lee *et al.* [13] studied the dilution effects of CO_2 on combustion instability and pollutant emissions, the flame temperature would decline when the dilution rate of CO_2 is rising, this will lead to the suppression of NO_x emissions and oscillation frequency. Zachary *et al.* [14] stabilized the unsteady flame with microjet air injection around the flame nozzle, they revealed that different modes of combustion instability will be observed, corresponding to particular flame shapes and resonant acoustic modes. Altay *et al.* [15] investigated the damping effectiveness of microjets in eliminating combustion instabilities. The microjets could change the shedding process of flame vortex, then the original phase relationship of flame-acoustic would be changed. Deshmukh and Sharma [16] eliminated thermoacoustic instability with methods of eight microjet holes around the Rijke tube. The effectiveness of control could be adjusted with different flame positions and JICF flow rates. Oztarlik *et al.* [17] shown that thermoacoustic instability can be stabilized even use very small flow rates of H_2 . But the concentration of CO or NO_x emissions will be drastically increase with some injection medium. Uhm and Acharya [18] demonstrated the effectiveness of high momentum air microjets in eliminating combustion instabilities. The phase relationship between flame and acoustic become mismatched thus changes the thermoacoustic interaction mechanism. Zhou *et al.* [19-21] suppressed the combustion instability with different microjets around the burner nozzles. The CO_2 , air and N_2 are employed as the injection medium. The experiments concluded that NO_x emissions can be reduced with N_2 , CO_2 , and CO_2/O_2 . Tao and Zhou [22] studied the effects of preheated oxy JICF on thermoacoustic instability and NO_x emissions. They revealed that the temperature of the CO_2/O_2 is essential for the control effectiveness of combustion dynamics and pollutant emissions. The aforementioned researches proved that the microjets around burner nozzle can effectively and conveniently control flame dynamics and pollutant emission pathways.

Although there are some control studies of JICF on combustion dynamics and pollutant formation pathways [14-22]. The influence of different injection medium on the control effectiveness of flame is far from thoroughly research. The difference in injection medium determines the chemical reaction process and physical change process of the unsteady flame. The flame adiabatic temperature and burning velocity can be changed under different oxidant atmosphere, thus the formation of active radicals during combustion was altered [23]. Flame structure and extinction limits also converted under different injection medium [24]. Besides,

the injection oxidant atmosphere changes the heat release rate and specific heat capacity of the flame. The ignition delays and chemical kinetics will be adjusted with different dilution gases [25-27]. The flame sensitivity and pollutant formation pathways under different dilution mediums cannot be ignored [28, 29]. As the JICF process involves multiple aspects: the thermal effects, the fuel compensation effects, the oxidation effects, the chemical effects, and the inertia effects [30, 31]. The flame stability limits under different JICF media need a further study [32]. The soot formation, quenching distances and minimum ignition energies can be optimized with different dilutions [33, 34]. The anchoring zones of the flame greatly depend on the composition-sensitive extinction strain rate of the mixture [35]. At the same time, the injection medium can significantly alter the dynamic characteristics of the lean premixed flame. The oxygen ratio of the dilution oxidant will exert impact on flame heat release rate and burning velocities [36]. Currently, although there are some literatures that studies the effects of CO₂, N₂, He, and Ar on the combustion reaction process [23-31]. Influence of the dilution oxidant: CO₂/O₂, N₂/O₂, and Ar/O₂ have profound impact of the regulation of combustion process [23, 27]. However, effects of the oxy (CO₂/O₂, N₂/O₂, Ar/O₂, and He/O₂) JICF on combustion dynamics and pollutant emissions have never been explored and compared. The flame and reacting flow stabilization characteristics under CO₂/O₂, N₂/O₂, Ar/O₂, and He/O₂ JICF need to be explored and summarized, thus combine the advantages of oxyfuel combustion into the damping of combustion instability or pollutant emissions.

This article aims to evaluate the oxy effects of CO₂/O₂, N₂/O₂, Ar/O₂, and He/O₂ JICF on combustion instability and NO_x emissions in a model lean premixed gas turbine combustor. The oxygen ratio and injection flow rate of the CO₂/O₂, N₂/O₂, Ar/O₂, and He/O₂ jets were varied during the experiments. Thus the control effectiveness of CO₂/O₂, N₂/O₂, Ar/O₂, and He/O₂ jets can be obtained and evaluated. Acoustic, heat release, NO_x emissions and image signals of flame were recorded. This study provides a new JICF control method for combustion dynamics and pollutant emissions, which will be contribute to the design of advanced combustors.

Experimental set-up

Geometry structure of the combustor

Figure 1 shows the geometry structure of the model lean premixed gas turbine combustor in this study. The detailed design of this combustor can be found in our previously published studies [19-22]. The whole combustor was composed of the gas premixed chamber (400 mm), the swirling section (100 mm), the quartz glass combustion chamber (300 mm), and the flue gas outlet section (315 mm). The inner diameter of all the four sections is set as 114 mm. A necking structure with height of 202 mm is preserved for loudspeaker connection, which can be used for the experiment of acoustic-excitation in the future. The CH₄ and air enters the premixed chamber through four air intake holes on the wall. Corrugated plates and honeycombs are installed in the premixed chamber for gas mixing. Figure 2 presents the 3-D cutaway views of the model gas turbine combustor, which contains the burner swirling section and the premixed chamber. The detailed geometrical structure of the bluff body and honeycombs are plotted. Honeycombs are installed at the downstream of the air intake holes. The dynamic pressure sensor on the combustion chamber is installed with the semi-infinite length method [20-22]. The swirl number of this lean premixed combustor is 1.152, the calculation process can be found in our previously published studies [19-22]. Sixteen straight axial vanes are used in the swirler. Flange is used for the connection of upstream and downstream of the burner. The outlet diameter of the burner nozzle is 20 mm, with a bluff body installed in the center for flame stabilization purpose.

The upstream diameter of the bluff body is 11 mm, the downstream diameter of the bluff body is 6 mm. The necking angle of the burner nozzle is 55° . According to the geometric parameters set previously, the cut-off frequency of the burner is 1510 Hz, this value is larger than the self-excited frequency of the combustor in this study (268 Hz). Hence the combustor can be treated as a 1-D tube, and the acoustic wave traveled in single direction.

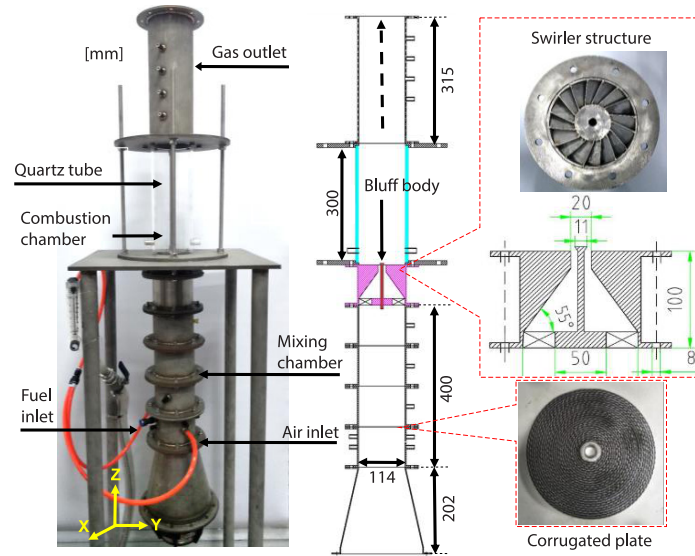


Figure 1. Geometry structure of the model lean premixed gas turbine combustor; the combustor was composed of premixed chamber, swirler, combustion chamber and flue gas outlet section [19-22]

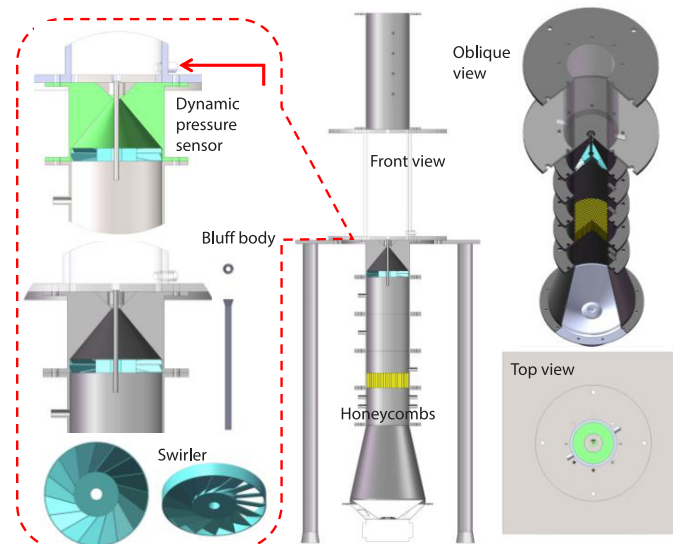


Figure 2. The cutaway view of the burner swirling section and the premixed chamber; the detailed geometrical structure of the bluff body and honeycombs are plotted [19-22]

Jet in cross-flow section

Figure 3 shows the geometrical structure of the CO₂/O₂, N₂/O₂, Ar/O₂, and He/O₂ JICF section applied in this study. Four injectors are implemented in the injection section, the inner diameter of each injector is set as 4 mm. The four injectors are arranged symmetrically at 90° around the wall of the injection section. The length of each injector is 25 mm from the inner wall of the injection section. The injection section is installed at the outlet of the burner nozzle, which is between the swirling section and the combustion chamber [20]. The injection medium flows in the injector and jets toward the anchoring zone of the flame root. The inner diameter of the injection section is 114 mm. The height of the injection section is 10 mm. In fig. 3, zero point of the Z co-ordinate axis is 5 mm from the outlet of the burner nozzle. Table 1 shows the experimental conditions of this research [19-22].

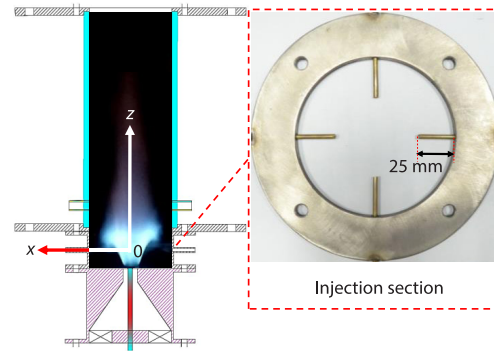


Figure 3. The geometrical structure of the JICF section; four injectors are used in this study, the inner diameter of each injector is 4 mm; the four injectors are arranged symmetrically at 90°

Table 1. Experimental conditions of this research

Parameters	Values
Thermal power [kW]	5.0
Equivalence ratio, Φ	0.70
Self-ex-cited condition	43.6 Pa, 268 Hz
Atmospheric pressure [MPa]	0.105
Ambient temperature [C°]	25
Relative humidity [%]	50-55
JICF rate [Lpm]	0.5, 1.0, 1.5, 2.0, 2.5, 3.0, 3.5
Oxygen ratio [%]	21, 27, 33, 39,45, 51
Injector numbers	4
JICF medium	CO ₂ /O ₂ , N ₂ /O ₂ , Ar/O ₂ , He/O ₂
Fuel type	CH ₄ , 99.995% purity

Measuring instruments

Figure 4 presents the measuring instruments of the experiments. Figure 4 contains the CO₂/O₂, N₂/O₂, Ar/O₂, and He/O₂ JICF system, the fuel/air supply system, the flue gas measuring system and the combustion dynamics recording system. The injection medium of CO₂, N₂, Ar, and He is supplied with high pressure tanks. Gaseous CO₂, N₂, Ar, and He is mixed with O₂ in a mixing chamber before injection. The flow rate of CO₂, N₂, Ar, He, and CH₄ can be regulated with the Alicat flow controller [19-22]. The oxygen ratio based on the volumetric flow rate of gas. Air is supplied with an air pump, which was adjusted with glass flowmeter. Testo 350 flue gas analyzer is applied for the testing of NO_x emissions, the measured NO_x value is corrected to 15% oxygen ratio in this study [20]. The acoustic wave signal of the flame is measured with two

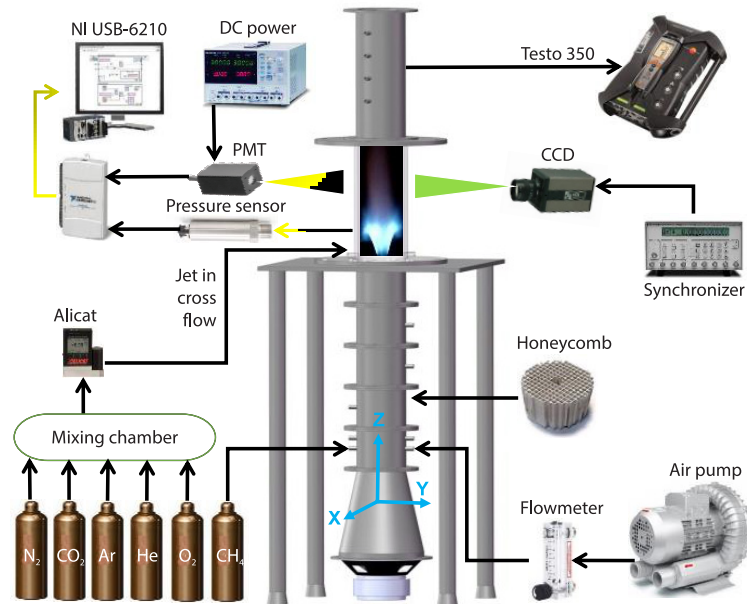


Figure 4. Measuring instruments for the experiments; which contains the CO_2/O_2 , N_2/O_2 , Ar/O_2 , and He/O_2 JICF system, the fuel/air supply system, the flue gas measuring system and the combustion dynamics recording system [19-22]

dynamic pressure sensors. The heat release rate can be reflected by measuring the CH^* signal of flame. The CH^* chemiluminescence signal is recorded with photomultiplier tube (PMT).

Results and discussions

Influence of JICF rates

Figure 5 shows the effect of different CO_2/O_2 , N_2/O_2 , Ar/O_2 , and He/O_2 JICF rate on the sound pressure amplitude measured in the combustion chamber, with the flow rate ranges from 0.5-3.5 Lpm, and the oxygen ratio is fixed at 21%. As the JICF injection flow rate increases, the sound pressure amplitude firstly increases and then decreases. Under the CO_2/O_2 JICF cases, the sound pressure amplitude firstly increases from 7.2-18.3 Pa, and finally declines to 12 Pa. Under the He/O_2 JICF cases, the sound pressure amplitude firstly increases from 30.4-46 Pa, and finally declines to 25.6 Pa. On the whole, CO_2/O_2 shows a better suppression effects than other three medium. The order of control effectiveness is $\text{CO}_2/\text{O}_2 > \text{Ar}/\text{O}_2 > \text{N}_2/\text{O}_2 > \text{He}/\text{O}_2$. Molecular masses determines the injection momentum ratio of JICF. Figure 5 manifested that the control effectiveness of CO_2/O_2 , N_2/O_2 , Ar/O_2 , and He/O_2 JICF will be deteriorated even with high flow rates. This may be due to the oxidization and thermal chemical effects that surpasses the JICF dilution effects during combustion. As the sound pressure increases to a peak value, the JICF dilution effects will exceed the oxidization and thermal chemical effects of the injection medium. Figure 6 shows the effects of different 'oxy' CO_2/O_2 , N_2/O_2 , Ar/O_2 , and He/O_2 JICF rate on the sound pressure frequency in the combustion chamber. The variation tendency is similar to the amplitude of sound pressure in fig. 5. When the combustion instability amplitude is high, the corresponding oscillation frequency is also high. Under the CO_2/O_2 JICF cases, the sound pressure frequency firstly increases from 260-266 Hz, and finally declines to 263 Hz. Under the He/O_2 JICF cases, the sound pressure frequency firstly increases from

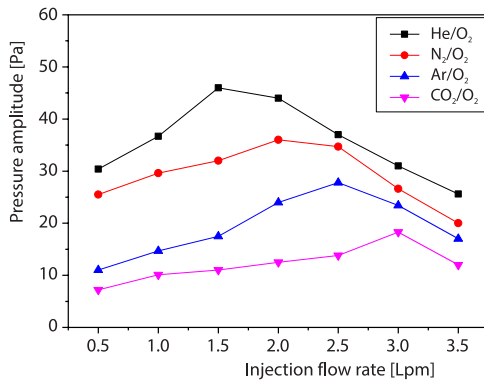


Figure 5. Effects of different CO₂/O₂, N₂/O₂, Ar/O₂, and He/O₂ JICF rate on the sound pressure amplitude in the combustion chamber, the flow rate ranges from 0.5-3.5 Lpm, and the oxygen ratio is 21%

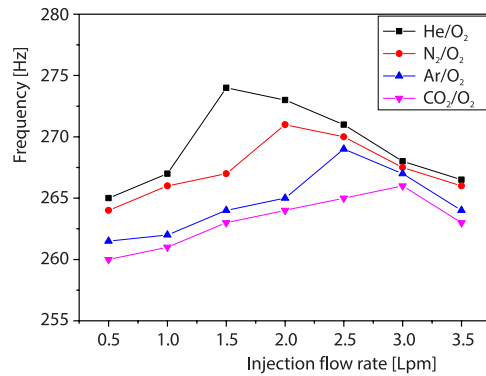


Figure 6. Effects of different CO₂/O₂, N₂/O₂, Ar/O₂, and He/O₂ JICF rate on the sound pressure frequency in the combustion chamber, the flow rate ranges from 0.5-3.5 Lpm, and the oxygen ratio is 21%

265-274 Hz, and finally declines to 267 Hz. The order of the average oscillation frequency is CO₂/O₂ > Ar/O₂ > N₂/O₂ > He/O₂. Figure 6 denotes that frequency shifting emerged during the dilution process. This is because the original interaction mechanism and phase relationship of acoustic-heat release was converted. Thus the coupling of combustion instability was broken.

Figure 7 shows the effect of different JICF rate on the CH* chemiluminescence amplitude of the flame. As the JICF injection flow rate gradually increases, the CH* chemiluminescence amplitude firstly increases and then decreases. Under the CO₂/O₂ JICF cases, the flame CH* chemiluminescence amplitude firstly increases from $3 \cdot 10^{-4}$ arb. units to $6.3 \cdot 10^{-4}$ arb. units, and finally declines to $2.8 \cdot 10^{-4}$ arb. units. Under He/O₂ JICF cases, the CH* chemiluminescence amplitude firstly increases from $1.75 \cdot 10^{-3}$ arb. units to $2.76 \cdot 10^{-3}$ arb. units, and finally declines to $1.52 \cdot 10^{-3}$ arb. units. The specific heat capacity and molecular radiation determines the flame heat release rate under different JICF cases. Effects of inertia atmosphere will exceed the effects of oxidization as the injection flow rate increases. Figure 8 shows the effects of different CO₂/O₂, N₂/O₂, Ar/O₂, and He/O₂ JICF rate on the CH* chemiluminescence

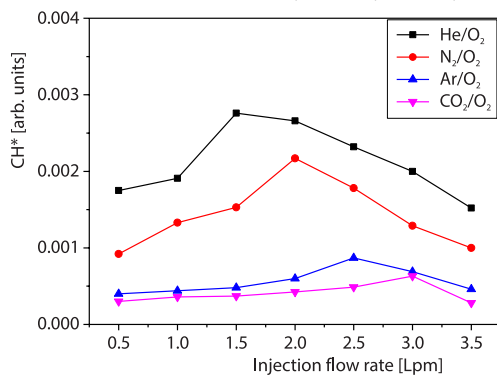


Figure 7. Effects of different CO₂/O₂, N₂/O₂, Ar/O₂, and He/O₂ JICF rate on the CH* chemiluminescence amplitude of the flame, the flow rate ranges from 0.5-3.5 Lpm, and the oxygen ratio is 21%

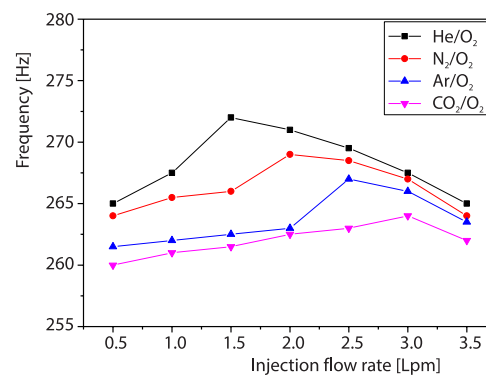


Figure 8. Effects of different CO₂/O₂, N₂/O₂, Ar/O₂, and He/O₂ JICF rate on the CH* chemiluminescence frequency of the flame, the flow rate ranges from 0.5-3.5 Lpm, and the oxygen ratio is 21%

frequency of the flame. This variation tendency is similar to the amplitude of flame CH^* chemiluminescence in fig. 7. When the flame CH^* chemiluminescence oscillation amplitude is high, the corresponding oscillation frequency of is also high. When under the CO_2/O_2 JICF cases, the CH^* chemiluminescence frequency firstly increases from 260-264 Hz, and finally declines to 262 Hz. Under He/O_2 JICF cases, the CH^* chemiluminescence frequency firstly increases from 265-272 Hz, and finally declines to 265 Hz. The order of the average CH^* chemiluminescence oscillation frequency is $\text{CO}_2/\text{O}_2 > \text{Ar}/\text{O}_2 > \text{N}_2/\text{O}_2 > \text{He}/\text{O}_2$. Figure 8 demonstrated that frequency switching emerged during the CO_2/O_2 , N_2/O_2 , Ar/O_2 and He/O_2 JICF dilution process. This can be attribute to the variation of chemical reaction pathways and burning velocities during the JICF dilution. The transformation process of the lean premixed flame under thermoacoustic instability is tightly associated with combustion kinetics, molecular dynamics and thermodynamics in the combustion chamber. These diluent gas have different specific heat capacity and thermal radiation, thus the 3-D temperature field of the combustion chamber was changed. In figs. 6 and 8, the effect of change in the diluent composition on the flame temperature may be another reason that affects NO_x emission.

Influence of JICF oxygen ratio

Figure 9 shows the influences of different CO_2/O_2 , N_2/O_2 , Ar/O_2 , and He/O_2 JICF oxygen ratio on the acoustic amplitude of the combustor. The JICF rate is kept constant at 2.0 Lpm, the oxygen ratio of the four injection medium ranges from 21-51%. As the oxygen ratio of the JICF gradually increases, the sound pressure amplitude firstly decreases during the oxygen ratio range of 21-33%. Then the sound pressure amplitude increases during the oxygen ratio range of 39-51%. Under the CO_2/O_2 JICF cases, the sound pressure amplitude firstly decreases from 12.5-8.3 Pa, and finally increases to 14.5 Pa. Under He/O_2 JICF cases, the sound pressure amplitude firstly drops from 44-26 Pa, and finally grows to 38 Pa. On the whole, the CO_2/O_2 case shows a better damping effects on combustion instability than other three injection medium. The order of control effectiveness can be sorted as $\text{CO}_2/\text{O}_2 > \text{Ar}/\text{O}_2 > \text{N}_2/\text{O}_2 > \text{He}/\text{O}_2$. The variation of oxygen ratio determines the combustion dynamics and burning velocity of unsteady flame. Figure 5 denotes that the control effective-

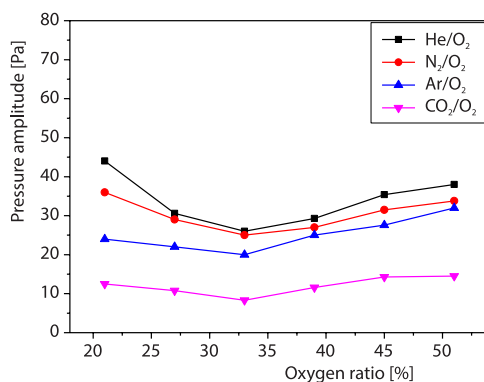


Figure 9. Effects of different CO_2/O_2 , N_2/O_2 , Ar/O_2 , and He/O_2 JICF oxygen ratio on the sound pressure amplitude in the combustion chamber, the flow rate is set as 2.0 Lpm, oxygen ratio of the injection medium ranged from 21-51%

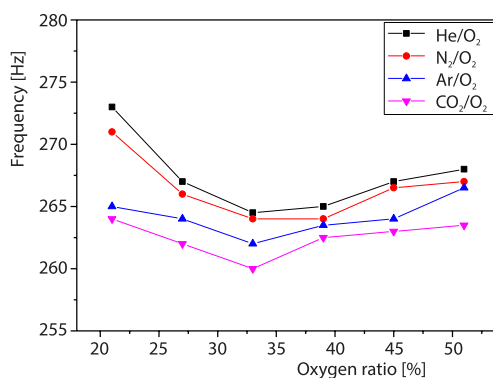


Figure 10. Effects of different CO_2/O_2 , N_2/O_2 , Ar/O_2 , and He/O_2 JICF oxygen ratio on the sound pressure frequency in the combustion chamber, the flow rate is set as 2.0 Lpm, oxygen ratio of the injection medium ranged from 21-51%

ness of CO_2/O_2 , N_2/O_2 , Ar/O_2 , and He/O_2 JICF is associated with oxygen ratio and the injection medium. As the injection flow rate keeps constant, although the oxygen ratio of the injection medium increases, the decreasing of sound pressure may be due to the oxidizer effects that below the JICF dilution effects. As the sound pressure amplitude drops to a lowest value, the oxidizer effects will exceed the JICF dilution effects from the injection medium. It is clearly presented in figs. 5 and 9, that there are turning points when eliminating combustion instability with different injection flow rate or oxygen ratios. Figure 10 shows the effects of different CO_2/O_2 , N_2/O_2 , Ar/O_2 , and He/O_2 JICF oxygen ratio on the oscillation frequency. The variation tendency of sound pressure frequency is similar to the amplitude of sound pressure in fig. 9. The variation trend of sound pressure frequency is also an inverted U-shape. Under the CO_2/O_2 JICF cases, the sound pressure frequency firstly decreases from 264-260 Hz, and finally declines to 264 Hz. Under He/O_2 JICF cases, the sound pressure frequency firstly decreases from 273-265 Hz, and finally increases to 268 Hz. The order of the average oscillation frequency of the four injection medium is $\text{CO}_2/\text{O}_2 > \text{Ar}/\text{O}_2 > \text{N}_2/\text{O}_2 > \text{He}/\text{O}_2$. Different oxygen ratio will cause the frequency switching of thermoacoustic instability. The original interaction mechanism and phase relationship of flame-acoustic-flow was transformed under oxy medium dilution. With the proper selection of oxygen ratio, flow rate and injection medium, an optimal can control effectiveness can be obtained.

Figure 11 shows the effect of different CO_2/O_2 , N_2/O_2 , Ar/O_2 , and He/O_2 JICF oxygen ratio on the CH^* chemiluminescence amplitude of the flame. As the oxygen ratio of JICF increases, the CH^* chemiluminescence amplitude firstly decreases during the oxygen ratio range of 21-33%. However, the CH^* chemiluminescence amplitude increases during the oxygen ratio range of 39-51%. Under CO_2/O_2 JICF cases, the CH^* chemiluminescence amplitude firstly decreases from $4.24 \cdot 10^{-4}$ arb. units to $3.3 \cdot 10^{-4}$ arb. units, and finally increases to $6.35 \cdot 10^{-4}$ arb. units. When under the He/O_2 JICF cases, the CH^* chemiluminescence amplitude firstly decreases from $2.66 \cdot 10^{-3}$ arb. units to $1.19 \cdot 10^{-3}$ arb. units, and finally declines to $1.67 \cdot 10^{-3}$ arb. units. It is the result of the combined influence of oxidant and inert jet gas, which changes flame heat releases rate with different oxygen content. Figure 12 shows the effects of different CO_2/O_2 , N_2/O_2 , Ar/O_2 , and He/O_2 JICF oxygen ratio on the CH^* chemiluminescence frequency of the flame. The variation trend of CH^* chemiluminescence frequency is an inverted

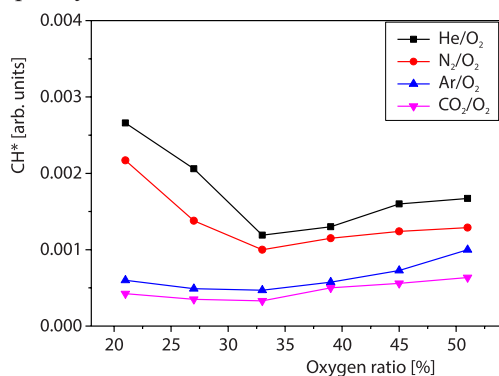


Figure 11. Effects of different CO_2/O_2 , N_2/O_2 , Ar/O_2 , and He/O_2 JICF oxygen ratio on the CH^* chemiluminescence amplitude of the flame, the flow rate is set as 2.0 Lpm, oxygen ratio of the injection medium ranged from 21-51%

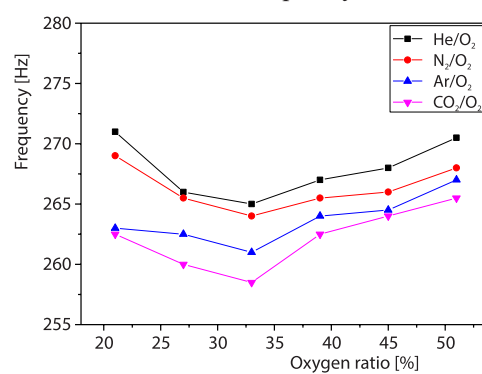


Figure 12. Effects of different CO_2/O_2 , N_2/O_2 , Ar/O_2 , and He/O_2 JICF oxygen ratio on the CH^* chemiluminescence frequency of the flame, the flow rate is set as 2.0 Lpm, oxygen ratio of the injection medium ranged from 21-51%

U-shape. The variation tendency of frequency is similar to the amplitude of CH^* chemiluminescence in fig. 11. Under the CO_2/O_2 JICF cases, the CH^* chemiluminescence frequency firstly drops from 263-259 Hz, and finally increases to 266 Hz. Under He/O_2 JICF cases, the CH^* chemiluminescence frequency firstly decreases from 271-265 Hz, and finally returns to 271 Hz. The order of the average CH^* chemiluminescence oscillation frequency is arranged as $\text{CO}_2/\text{O}_2 > \text{Ar}/\text{O}_2 > \text{N}_2/\text{O}_2 > \text{He}/\text{O}_2$. Figure 12 demonstrated that the frequency switching of CH^* chemiluminescence also emerged when the oxygen ratio of the JICF varied. This is because under the atmosphere of different oxidants, the free chemical radicals and atomic radiations during the combustion process may be changed, which leads to the appearance of mode migrations on flame heat release rate.

The NO_x emission characteristics

Figure 13 shows the effect of different CO_2/O_2 , N_2/O_2 , Ar/O_2 , and He/O_2 JICF rate on the concentration of NO_x emissions, the oxygen ratio of JICF is fixed at 21%, and the flow rate of JICF ranges from 0.5-3.5 Lpm. As the JICF injection flow rate increases, the concentration of NO_x emissions gradually declines. The NO_x emission concentration before using the JICF is 25.5 ppm. Under the CO_2/O_2 JICF cases, the NO_x emission concentration decreases from 22.3-15.2 ppm, the damping ratio of NO_x is 40.39%. Under He/O_2 JICF cases, the NO_x emission concentration drops from 23-16.5 ppm, the damping ratio of NO_x is 35.29%. The CO_2/O_2 JICF could achieve a better suppression effects than the other three medium. The control effectiveness of the NO_x emission concentration is $\text{CO}_2/\text{O}_2 > \text{Ar}/\text{O}_2 > \text{N}_2/\text{O}_2 > \text{He}/\text{O}_2$. The difference in molecular masses and injection flow rate determines the injection momentum ratio of the four injection medium. Thus the CO_2/O_2 JICF with higher relative molecular masses could penetrate the flame anchoring zones easily. The flame temperature becomes more uniform and the number of hot spot in the combustion chamber can be reduced, which will get a better NO_x emission control results. The He/O_2 JICF with lower relative molecular masses could not penetrate the flame anchoring zones easily, thus the temperature field of the combustion chamber has not changed much. Compared fig. 5 with fig. 13, under different injection flow rates, the changing trends of pollutant emissions and combustion instability are inconsistent.

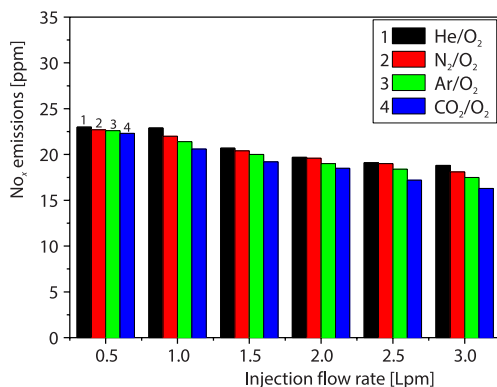


Figure 13. Effects of different CO_2/O_2 , N_2/O_2 , Ar/O_2 , and He/O_2 JICF rate on the concentration of NO_x emission, the flow rate ranges from 0.5-3.5 Lpm, and the oxygen ratio is 21%

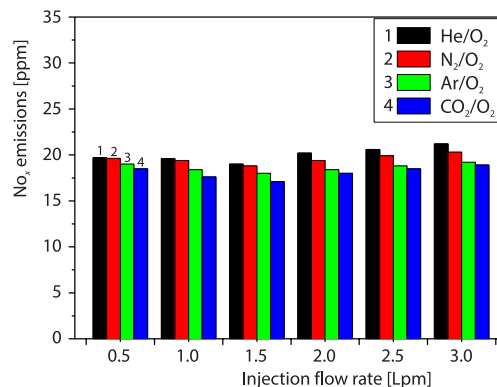


Figure 14. Effects of different CO_2/O_2 , N_2/O_2 , Ar/O_2 , and He/O_2 JICF oxygen ratio on the concentration of NO_x emission, the flow rate is set as 2.0 Lpm, oxygen ratio of the injection medium ranged from 21-51%

Figure 14 shows the effects of different CO_2/O_2 , N_2/O_2 , Ar/O_2 , and He/O_2 JICF oxygen ratio on the concentration of NO_x emission, the oxygen ratio of the injection medium ranged from 21-51%, and the JICF flow rate is set as 2.0 Lpm. As the oxygen ratio of JICF increases, the concentration of NO_x emissions firstly decreases during the oxygen ratio range of 21-33%. However, the concentration of NO_x emissions then increases during the oxygen ratio range of 39-51%. Under the He/O_2 JICF cases, the NO_x emission concentration firstly decreases from 19.7-19 ppm during the oxygen ratio of 21-33%, then increases to 21.2 ppm during the oxygen ratio range of 39-51%. Under the CO_2/O_2 JICF cases, the NO_x emission concentration firstly drops from 18.5-17.1 ppm during the oxygen ratio range of 21-33%, then increases to 18.9 ppm during the oxygen ratio range of 39-51%. The CO_2/O_2 JICF could achieve a better suppression effects than the other three medium. The control effectiveness of NO_x emission concentration is $\text{CO}_2/\text{O}_2 > \text{Ar}/\text{O}_2 > \text{N}_2/\text{O}_2 > \text{He}/\text{O}_2$. Except for the dilution impacts, the methane and oxygen mass fractions may be the reason lead to the variation of NO_x emissions.

Variation of flame structures

Figure 15 shows the effects of different CO_2/O_2 , N_2/O_2 , Ar/O_2 , and He/O_2 JICF rate on the macro-structures of lean premixed flames. The flow rate of JICF ranges from 0.5-3.5 Lpm, the oxygen ratio is set as 21%. As the JICF injection flow rate increases, the macro-structure of the flame gradually changes. The flame gradually shortens as the JICF rate increases from 0.5-3.5 Lpm. Under the CO_2/O_2 JICF cases, the flame have long and red fronts, which gradually disappears as the injection flow rate increases. Under He/O_2 JICF cases, the flame have no fronts. The corresponding flame length is calculated and presented in fig. 17 He/O_2 JICF could achieve a lower flame length than the other three medium. The reduction of flame length is sorted as $\text{He}/\text{O}_2 > \text{N}_2/\text{O}_2 > \text{Ar}/\text{O}_2 > \text{CO}_2/\text{O}_2$. The flame length declined from 105-67 mm under the CO_2/O_2 JICF cases. The flame length declined from 73-41 mm under the He/O_2 JICF cases. The application of oxy JICF will bring better mixing and higher burning velocity for the flame. Due to the overall increasing of chemical reaction rate of lean premixed flame. The relative residence time of flame in the combustion chamber will decrease. Thus the reduction of flame length will realized.

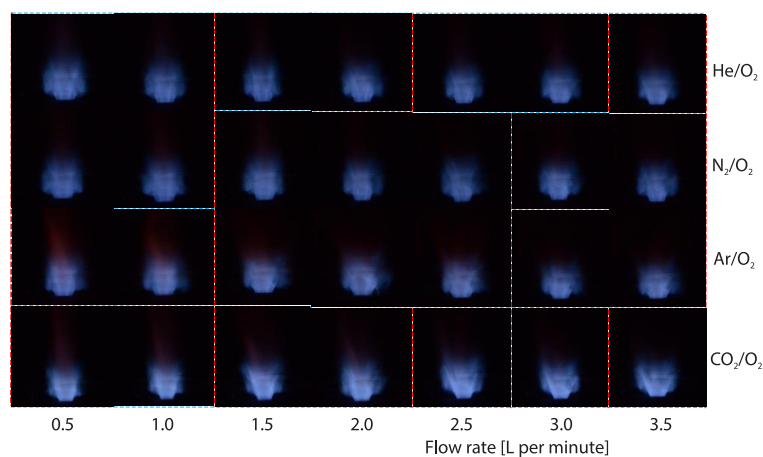


Figure 15. Effects of different CO_2/O_2 , N_2/O_2 , Ar/O_2 , and He/O_2 JICF rate on the flame shape, the flow rate ranges from 0.5-3.5 Lpm, the oxygen ratio is set as 21%

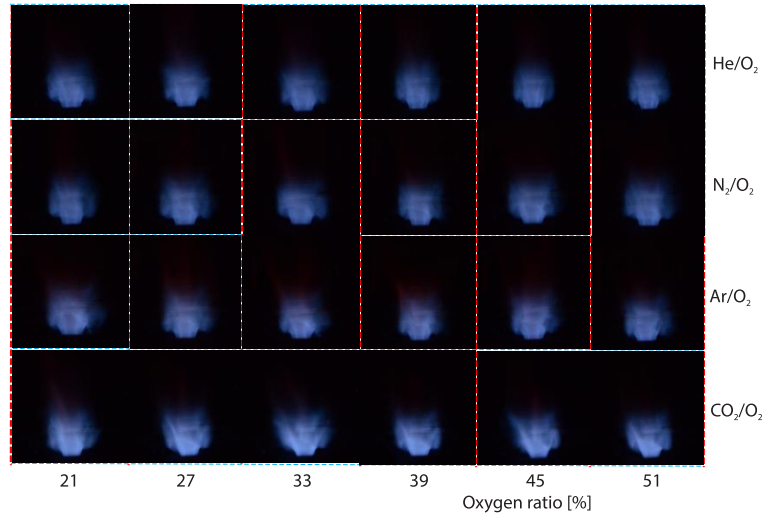


Figure 16. Effects of different CO_2/O_2 , N_2/O_2 , Ar/O_2 , and He/O_2 JICF oxygen ratio on the flame shape, the injection flow rate is set as 2.0 Lpm, oxygen ratio of the injection ranged from 21-51%

Figure 16 presents the effects of different CO_2/O_2 , N_2/O_2 , Ar/O_2 , and He/O_2 JICF oxygen ratio on the flame shape, the injection flow rate is set as 2.0 Lpm, oxygen ratio of the injection medium ranged from 21-51%. As the oxygen ratio of the JICF increases, the macro-structure of the flame gradually changes. The flame gradually stretches during the oxygen ratio of 21-33%, then the flame shortens during the oxygen ratio of 39-51%. Under the CO_2/O_2 , N_2/O_2 , and Ar/O_2 JICF cases, the flame fronts firstly emerged and then disappeared as the oxygen ratio increases. The corresponding flame length of fig. 16 is calculated and presented in fig. 18. The JICF cases of He/O_2 could achieve a lower flame length than the other three medium. The reduction degree of flame length is sorted as $\text{He}/\text{O}_2 > \text{N}_2/\text{O}_2 > \text{Ar}/\text{O}_2 > \text{CO}_2/\text{O}_2$. Under the CO_2/O_2 JICF cases, the length of the flame gradually rises from 94 mm to 99.5 mm

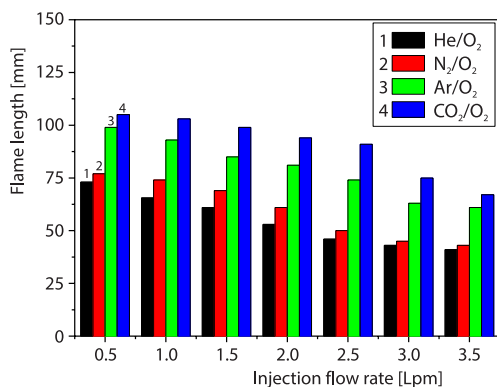


Figure 17. Effects of different CO_2/O_2 , N_2/O_2 , Ar/O_2 , and He/O_2 JICF rate on the flame length, the flow rate ranges from 0.5-3.5 Lpm, oxygen ratio of the injection medium set as 21%

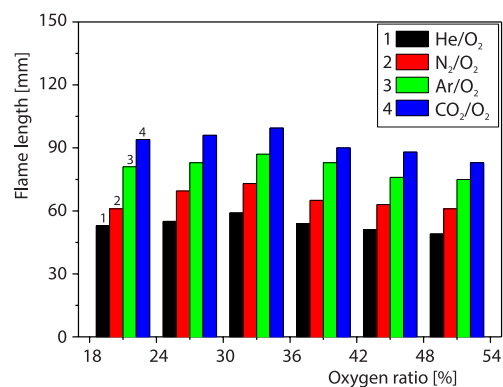


Figure 18. Effects of different CO_2/O_2 , N_2/O_2 , Ar/O_2 , and He/O_2 JICF oxygen ratio on the flame length, the injection flow rate is set as 2.0 Lpm, oxygen ratio of the injection medium ranged from 21-51%

during the oxygen ratio of 21-33 %, then the flame length declines to 83 mm during the oxygen ratio of 39-51%. Under the He/O₂ JICF cases, the flame length gradually increases from 53-59 mm during the oxygen ratio of 21-33%, then the flame length declines to 49 mm during the oxygen ratio of 39-51%. Different oxygen ratio affects the flame burning velocities, resulting in the flame stretching rate being changed. The internal and external re-circulation region being changed with different JICF dilutions.

Conclusions

This study experimentally investigated the performance of the oxy CO₂/O₂, N₂/O₂, Ar/O₂, and He/O₂ JICF on combustion instability and NO_x emissions. The study was carried out in a model gas turbine combustor. The non-linear influence of oxygen ratio and flow rates are revealed in this research. Some findings on the passive suppression of combustion instability and NO_x emissions with oxy JICF were demonstrated in the experimental results.

Although effective in eliminating combustion instability, the passive method of JICF is far from thoroughly researched. The physical and chemical variables of JICF could exert profound influences on combustion instability. If the relevant variables of JICF are not selected properly, it will cause the combustion oscillations more seriously. The quantitative and qualitative impact of JICF on combustion need a further study thus reveal the coupling or decoupling mechanism of thermoacoustic instability.

The variation of NO_x emissions is related to several interdisciplinary regions. During the process of JICF dilution, the free radicals and formation pathway of NO_x can be varied. The exactly reaction mechanism is important for understanding the NO_x emissions suppression process. The exactly weights of the injection flow rate, the oxygen ratio and the injection medium on pollutant emission have never been computed. The calculation of these weights can promote the control of NO_x emissions.

The macro-structure structure and length of flame are important indicators of stabilized combustion. The flame become more compact and short after JICF dilution, which helps in the decoupling process of flame-acoustic interaction. Advanced instruments such as the particle image velocimetry and planar laser induced fluorescence will be used in the future. Thus the chemical free radicals and flow field properties of flame under CO₂/O₂, N₂/O₂, Ar/O₂, and He/O₂ JICF can be illuminated.

Acknowledgment

This work was supported by the National Science Fund for Distinguished Young Scholars [No. 51825605] of China.

References

- [1] Huang, Y., Yang, V., Dynamics and Stability of Lean-Premixed Swirl-Stabilized Combustion, *Progress in Energy and Combustion Science*, 35 (2009), 4, pp. 293-364
- [2] Connor, J., *et al.*, Transverse Combustion Instabilities: Acoustic, Fluid Mechanic, and Flame Processes, *Progress in Energy and Combustion Science*, 49 (2015), Aug., pp. 1-39
- [3] Kim Y., *et al.*, Experimental Study on Combustion Instability and Attenuation Characteristics in the Lab-scale Gas Turbine Combustor with a Sponge-Like Porous Medium, *Journal of Mechanical Science and Technology*, 32 (2018), 4, pp. 1879-1887
- [4] Lee, D., Lee, C., Equivalence Ratio Variation and Combustion Instability in Hybrid Rocket, *Journal of Mechanical Science and Technology*, 33 (2019), 10, pp. 5033-5042
- [5] Pyo, Y., *et al.*, Numerical Investigation on Combustion Instability Modelling in a Lean Premixed Gas Turbine Combustor Combining Finite Element Analysis with Local Flame Transfer Function, *Journal of Mechanical Science and Technology*, 33 (2019), Nov., pp. 5547-5559

- [6] Cha, D., et al., Analysis of the Combustion Instability of a Model Gas Turbine Combustor by the Transfer Matrix Method, *Journal of Mechanical Science and Technology*, 23 (2009), 6, pp. 1602-1612
- [7] Lee, C., et al., Numerical Study of the Effect of Inlet Geometry on Combustion Instabilities in a Lean Premixed Swirl Combustor, *Journal of Mechanical Science and Technology*, 30 (2016), 11, pp. 5293-5303
- [8] Yoon, J., et al., Instability Mode and Flame Structure Analysis of Various Fuel Compositions in a Model Gas Turbine Combustor, *Journal of Mechanical Science and Technology*, 29 (2015), 3, pp. 899-907
- [9] Seo, S., et al., Analysis of the Combustion Oscillation in a Silo-Type Gas Turbine Combustor and Its Suppression, *Journal of Mechanical Science and Technology*, 26 (2012), 4, pp. 1235-1240
- [10] Yoon, M., Kim, D., Acoustic Transfer Function of a Combustion System with Premixing Chamber, *Journal of Mechanical Science and Technology*, 31 (2017), 12, pp. 6069-6076
- [11] Zhao, D., et al., A Review of Active Control Approaches in Stabilizing Combustion Systems in Aerospace Industry, *Progress in Aerospace Sciences*, 97 (2018), Feb., pp. 35-60
- [12] Zhao, D., Li, X., A Review of Acoustic Dampers Applied to Combustion Chambers in Aerospace Industry, *Progress in Aerospace Sciences*, 74 (2015), Apr., pp. 114-130
- [13] Lee, K., et al., The CO₂ Radiation Heat Loss Effects on NO_x Emissions and Combustion Instabilities in Lean Premixed Flames, *Fuel*, 106 (2013), Complet, pp. 682-689
- [14] Zachary, B., et al., Flow Structures in a Lean-Premixed Swirl-Stabilized Combustor with Microjet Air Injection, *Proceedings of the Combustion Institute*, 33 (2011), 1, pp. 1575-1581
- [15] Altay, H., et al., Mitigation of Thermoacoustic Instability Utilizing Steady Air Injection Near the Flame Anchoring Zone, *Combustion and Flame*, 157 (2010), 4, pp. 686-700
- [16] Deshmukh, N., Sharma, S., Suppression of Thermo-Acoustic Instability Using Air Injection in Horizontal Rijke Tube, *Journal of the Energy Institute*, 90 (2017), 3, pp. 485-495
- [17] Oztarlik, G., et al., Suppression of Instabilities of Swirled Premixed Flames with Minimal Secondary Hydrogen Injection, *Combustion and Flame*, 214 (2020), Apr., pp. 266-276
- [18] Uhm, J., Acharya, S., Role of Low-Bandwidth Open-Loop Control of Combustion Instability Using a High Momentum Air Jet – Mechanistic Details, *Combustion and Flame*, 147 (2006), 1-2, pp. 22-31
- [19] Zhou, H., et al., Control of Thermoacoustic Instabilities by CO₂ and N₂ Jet in Cross-Flow, *Applied Thermal Engineering*, 36 (2012), 1, pp. 353-359
- [20] Zhou, H., Tao, C., Effects of Annular N₂/O₂ and CO₂/O₂ Jets on Combustion Instabilities and NO_x Emissions in Lean-Premixed Methane Flames, *Fuel*, 263 (2020), Nov., 116709
- [21] Zhou, H., et al., Optimal Control of Turbulent Premixed Combustion Instability with Annular Micropore Air Jets, *Aerospace Science and Technology*, 98 (2020), Mar., 105650
- [22] Tao, C. F., Zhou, H., Effects of Different Preheated CO₂/O₂ Jet in Cross-Flow on Combustion Instability and Emissions in a Lean-Premixed Combustor, *Journal of the Energy Institute*, 93 (2020), 6, pp. 2334-2343
- [23] Xiang, L., et al., Numerical Study on CH₄ Laminar Premixed Flames for Combustion Characteristics in the Oxidant Atmospheres of N₂/CO₂/H₂O/Ar-O₂, *Journal of the Energy Institute*, 93 (2020), 4, pp. 1278-1287
- [24] Zhao, X., et al., Effects of N₂ and CO₂ Dilution on the Combustion Characteristics of C₃H₈/O₂ Mixture in a Swirl Tubular Flame Burner, *Experimental Thermal and Fluid Science*, 100 (2019), Sept., pp. 251-258
- [25] Xiong, X., et al., Shock Tube Evaluation on C₂H₄ Ignition Delay Differences among N₂, Ar, He, CO₂ Diluent Gases, *Journal of the Energy Institute*, 93 (2020), 4, pp. 1271-1277
- [26] Mao, X., et al., Methane Pyrolysis with N₂/Ar/He Diluents in a Repetitively Pulsed Nanosecond Discharge: Kinetics Development for Plasma Assisted Combustion and Fuel Reforming, *Energy Conversion and Management*, 200 (2019), Nov., 112018
- [27] Xia, W., et al., Shock Tube and Modelling Study of Ignition Delay Times of Propane under O₂/CO₂/Ar Atmosphere, *Combustion and Flame*, 220 (2020), Oct., pp. 34-48
- [28] Kishore, V., et al., Adiabatic Burning Velocity of H₂-O₂ Mixtures Diluted with CO₂/N₂/Ar, *International Journal of Hydrogen Energy*, 34 (2009), 19, pp. 8378-8388
- [29] He, Y., et al., Comparison of the Characteristics and Mechanism of CO Formation in O₂/N₂, O₂/CO₂ and O₂/H₂O Atmospheres, *Energy*, 141 (2017), Dec., pp. 1429-1438
- [30] Yilmaz, H., Yilmaz, I., Effects of Synthetic Gas Constituents on Combustion and Emission Behavior of Premixed H₂/CO/CO₂/CNG Mixture Flames, *Journal of the Energy Institute*, 92 (2019), 4, pp. 1091-1106
- [31] Li, W., et al., Experimental and Theoretical Analysis of Effects of N₂, O₂ and Ar in Excess Air on Combustion and NO_x Emissions of a Turbocharged NG Engine, *Energy Conversion and Management*, 97 (2015), June, pp. 253-264

- [32] Esclapez, L., *et al.*, Fuel Effects on Lean Blow-out in a Realistic Gas Turbine Combustor, *Combustion and Flame*, 181 (2017), July, pp. 82-99
- [33] Chen, M., *et al.*, Soot Formation and Combustion Characteristics in Confined Mesoscale Combustors under Conventional and Oxy-Combustion Conditions (O_2/N_2 and O_2/CO_2), *Fuel*, 264 (2020), Mar., 116808
- [34] Movileanu, C., *et al.*, Quenching Distances, Minimum Ignition Energies and Related Properties of Propane Air Diluent Mixtures, *Fuel*, 274 (2020), Aug., 117836
- [35] Karlis, E., *et al.*, Effects of Inert Fuel Diluents on Thermoacoustic Instabilities in Gas Turbine Combustion, *AIAA Journal*, 58 (2020), 6, pp. 2643-2657
- [36] Shi, B., *et al.*, Carbon Dioxide Diluted Methane/Oxygen Combustion in a Rapidly Mixed Tubular Flame Burner, *Combustion and Flame*, 162 (2015), 2, pp. 420-430